JOURNAL OF BACTERIOLOGY, July 2010, p. 3512–3523 Vol. 192, No. 13
0021-9193/10/$12.00 doi:10.1128/JB.00258-10

Functional Characterization of *Synechocystis* sp. Strain PCC 6803 *pst1* and *pst2* Gene Clusters Reveals a Novel Strategy for Phosphate Uptake in a Freshwater Cyanobacterium▽

Frances D. Pitt, Sophie Mazard, Lee Humphreys, and David J. Scanlan*

Department of Biological Sciences, University of Warwick, Coventry CV4 7AL, United Kingdom

Received 9 March 2010/Accepted 23 April 2010

***Synechocystis* sp. strain PCC 6803 possesses two putative ABC-type inorganic phosphate (P_i) transporters with three associated P_i-binding proteins (PBPs), SphX (encoded by *sll0679*), PstS1 (encoded by *sll0680*), and PstS2 (encoded by *slr1247*), organized in two spatially discrete gene clusters, *pst1* and *pst2*. We used a combination of mutagenesis, gene expression, and radiotracer uptake analyses to functionally characterize the role of these PBPs and associated gene clusters. Quantitative PCR (qPCR) demonstrated that *pstS1* was expressed at a high level in P_i-replete conditions compared to *sphX* or *pstS2*. However, a P_i stress shift increased expression of *pstS2* 318-fold after 48 h, compared to 43-fold for *pstS1* and 37-fold for *sphX*. A shift to high-light conditions caused a transient increase of all PBPs, whereas N stress primarily increased expression of *sphX*. Interposon mutagenesis of each PBP demonstrated that disruption of *pstS1* alone caused constitutive expression of *pho* regulon genes, implicating PstS1 as a major component of the P_i sensing machinery. The *pstS1* mutant was also transformation incompetent. $^{32}P_i$ radiotracer uptake experiments using *pst1* and *pst2* deletion mutants showed that Pst1 acts as a low-affinity, high-velocity transporter (K_s, 3.7 ± 0.7 μM; V_{max}, 31.18 ± 3.96 fmol cell^{-1} min^{-1}) and Pst2 acts as a high-affinity, low-velocity system (K_s, 0.07 ± 0.01 μM; V_{max}, 0.88 ± 0.11 fmol cell^{-1} min^{-1}). These P_i ABC transporters thus exhibit differences in both kinetic and regulatory properties, the former trait potentially dramatically increasing the dynamic range of P_i transport into the cell, which has potential implications for our understanding of the ecological success of this key microbial group.**

Phosphorus input into aquatic systems is largely in the form of poorly soluble, eroded mineral phosphate, which enters these systems via runoff from land, making P_i a key growth-limiting nutrient, particularly in freshwater environments (13, 23, 41). A recent survey of 34 inland lakes from three (physiographic) regions of Canada (25) revealed total P_i concentrations ranging between 0.058 and 7.64 μM. Thus, organisms occupying such environments invariably need to make key biochemical and regulatory adaptations to their P_i uptake system in order to sustain growth. One such group is the cyanobacteria, one of the largest, most diverse, and most widely distributed prokaryotic lineages (42). Their ability to acclimate to a varying-light environment as well as their ability to acquire nutrients present at low ambient concentrations has led to their present-day dominance in vast tracts of oligotrophic open ocean waters (40) and in freshwater systems (14).

Studies of bacterial P_i acquisition have largely focused on model organisms such as *Escherichia coli* (52) and *Bacillus subtilis* (26). In *E. coli*, uptake utilizes both a low-affinity permease, the Pit system (54) [with uptake of P_i being reliant on cotransport with divalent metal cations such as Mg(II) or Ca(II) through the formation of a soluble, neutral metal-phosphate complex, which is then the transported species (28, 49)] and a high-affinity Pst transport system (52). The Pst transporter comprises a periplasmic P_i-binding protein (PstS), two integral membrane proteins (PstA and PstC), and an ATP-binding protein (PstB) (10, 44). Regulation of this complex is dependent on a two-component system encoded by the *phoBR* operon (31). In addition, the Pst system itself seems to play a role in regulation, with mutations in genes of the *pst* operon leading to constitutive expression of the *pho* regulon (52). Thus, the periplasmic PstS, which binds P_i with high affinity, could potentially act as the primary sensor of external P_i. Once loaded with P_i, PstS interacts with membrane components of the Pst system, causing a conformational change which is sensed by the PhoU protein, not involved in P_i transport (51). However, increased activity of the Pit transporters PitA and PitB can alleviate constitutive expression of the *pho* regulon and restore P_i regulation of the regulon (24).

In the freshwater cyanobacterium *Synechocystis* sp. strain PCC 6803 (herein, *Synechocystis*), while orthologs of the PhoB/R two-component system have been identified and the system has been shown to be exclusively responsible for the specific P_i limitation response (45), there are several features of the P_i acquisition system which are unusual and warrant further investigation. Firstly, *Synechocystis*, like several other freshwater strains (43) and most marine picocyanobacteria (40), contains no identifiable Pit transporter. In contrast, there are two gene clusters encoding potential ABC transporters for P_i (Fig. 1), which we designate here *pst1* and *pst2*, with three associated P_i-binding proteins (PBPs) (2, 32). *sll0540*, which encodes a fourth PBP, has also been identified in the *Synechocystis* genome, but its PBP is not colocalized with either *pst1* or *pst2*. Indeed, *pho* regulon predictions of several cyanobacterial genomes showed that 50% of freshwater strains contain "duplicate" *pst* transporters (43), while many freshwater and ma-

* Corresponding author. Mailing address: Department of Biological Sciences, University of Warwick, Coventry CV4 7AL, United Kingdom. Phone: 44 (0)24 76 52 8363. Fax: 44 (0)24 76 52 3701. E-mail: D.J.Scanlan@warwick.ac.uk.

▽ Published ahead of print on 30 April 2010.

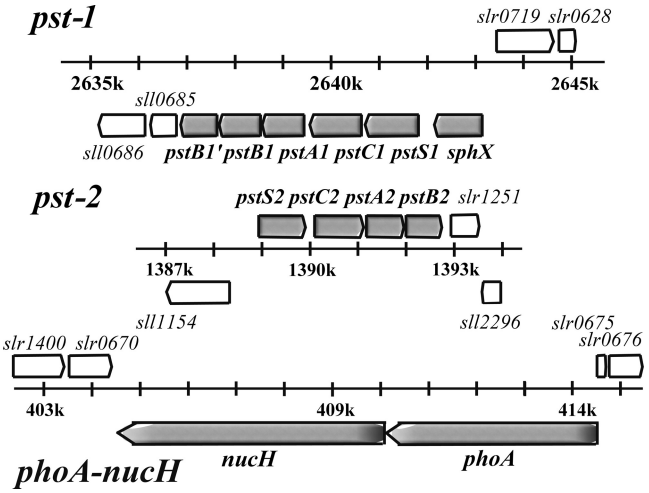

FIG. 1. Schematic representation of the two ABC P_i transporters and the *phoA-nucH* gene clusters.

rine strains contain multiple associated PBPs (40, 43). However, despite clear evidence of multiple P_i transport elements in cyanobacteria, little is known of the functional significance of individual, and apparently redundant, components of the cyanobacterial *pho* regulon.

Here, we assessed the role of multiple P_i transporter elements in *Synechocystis* by creating both mutants with complete deletions of the *pst1* and *pst2* gene clusters and single interposon mutants with mutations of the associated *pstS* and *sphX* genes. We generated gene expression profiles using quantitative PCR (qPCR) to analyze both wild-type (WT) and specific interposon mutants, under P_i-replete, P_i stress, and nitrate (N) stress conditions, as well as following a shift to high light. We show that disruption of *pstS1* (*sll0680*) leads to constitutive *pho* regulon gene expression consistent with PstS1 as a primary component of the P_i sensor. Such a phenotype is not observed in the *pstS2* (*slr1247*) and *sphX* (*sll0679*) mutants. Moreover, using radiotracer incorporation studies with *pst* gene cluster deletion mutants, we show that while both systems transport P_i, there are dramatic differences in their maximum uptake rates (V_{max}) and half-saturation constants (K_s) for P_i. These data demonstrate a novel strategy for P_i acquisition in a freshwater cyanobacterium.

MATERIALS AND METHODS

Culture growth conditions. Axenic cultures of *Synechocystis* sp. PCC 6803 WT and mutant strains were grown in BG-11 medium (38) at 30°C with shaking under continuous white light illumination (30 μmol photons m^{-2} s^{-1}). *Synechocystis* mutants were maintained in liquid BG-11 medium containing the appropriate antibiotic as follows: 50 μg ml^{-1} spectinomycin, 50 μg ml^{-1} apramycin, or 2.5 μg ml^{-1} gentamicin. For the P_i-free and N-free BG-11 media, $K_2HPO_4 \cdot 3H_2O$ and nitrate, respectively, were replaced by an equimolar amount of KCl. For the RNA work, cyanobacterial cultures (3 liters) were grown in BG-11 medium supplemented with 0.1% (wt/vol) sodium hydrogen carbonate, stirred continuously, and bubbled with air. In order for P_i stress conditions to be established in each time course, a 3-liter preculture was grown to an optical density at 750 nm (OD_{750}) of 0.5. The culture was then pelleted via centrifugation at 4,754 × *g* for 10 min and resuspended in 200 ml of P_i-free BG-11 medium. This washing process was repeated three times in order to remove any excess phosphate from the medium. The culture was then transferred into 3 liters of P_i-free BG-11 medium to give an OD_{750} of 0.3, and this was recorded as time point 0. *Synechocystis* cell samples were taken for RNA extraction, alkaline phosphatase (AP) activity measurement, and cell counts by using flow cytometry at various time points up to 48 h. During the shift to high light, in which cells were exposed to 600 μmol photons m^{-2} s^{-1} for a 24-h period, an OD_{750} of 0.08 was used in order to prevent self-shading of the culture during the time course. For $^{32}P_i$ radiotracer uptake, cells were grown in 100 ml BG-11 medium to an OD_{750} of 0.3, prior to the establishment of P_i stress conditions as described above. The culture was then left to shake for 48 h to allow recovery from centrifugation and to induce maximal gene expression in response to P_i stress. Cultures were then diluted to an OD_{750} of 0.08 in P_i-free BG-11 medium, and $^{32}P_i$ radiotracer uptake was assessed.

Phylogenetic and bioinformatic analyses. All sequences used for the analyses were extracted from GenBank (www.ncbi.nlm.nih.gov; accession numbers are shown in Table 1). The presence of a signal peptide cleavage site in the native protein chain was predicted by three algorithms: neural network, hidden Markov model (using the SignalP 3.0 server [http://www.cbs.dtu.dk/services/SignalP/]), and SigCleave from the EMBOSS suite (http://emboss.sourceforge.net/). The molecular weights and isoelectric points of PBPs were determined for the mature sequence, i.e., after removal of the predicted signal peptide by using the Pepstats program from EMBOSS. Phylogenetic analyses were conducted from an alignment of the amino acid sequences of the mature PstS and SphX from marine and freshwater cyanobacteria by using ClustalX v1.83 (47). The phylogenetic tree was constructed using the neighbor-joining algorithm and rooted on the PstS sequence of *Escherichia coli*. Bootstrap values were obtained through 1,000 repetitions.

Single-gene disruption mutants. *Synechocystis sll0679* (*sphX*), *sll0680* (*pstS1*), and *slr1247* (*pstS2*) mutants were constructed by interposon mutagenesis by using specific antibiotic resistance cassettes. Primers designed to target the flanking regions of the genes were *sphX*exF (5′-GCGCCTTCAGCCTGGACTGT-3′), *sphX*exR (5′-CTGGCCACGGCCACGATCAA-3′), *pstS1*exF (5′-AAGCCGTC AGAGTTTGTTTG-3′), *pstS1*exR (5′-TTCCCGCACATTTTGAGGTA-3′), *pstS2*exF (5′-CGACCAATTACTTGCCGGCT-3′), and *pstS2*exR (5′-CGGGCA TCGGTAAAAACCAC-3′). PCR was performed as follows: an initial denaturation at 98°C for 2 min was followed by 25 cycles of 95°C for 45 s, 45°C for 45 s, and 68°C for 3 min, followed by a final extension of 68°C for 5 min. Each 50-μl PCR mix contained 1 μM primers, 100 ng *Synechocystis* genomic DNA, 1× Promega PCR master mix reaction buffer. *sphX* and *pstS1* PCR products were then ligated into pCR2.1-TOPO vector (Invitrogen, United States), resulting in constructs pLH0679 (*sphX*) and pLH0680 (*pstS1*), and the *pstS2* product was ligated into LITMUS 38i vector (NEB), giving pLH1247lit38 (*pstS2*). pLH0679 and pLH0680 were digested with HincII and HpaI, respectively. This removed 824-bp and 108-bp internal fragments of the *sphX* and *pstS1* genes, respectively. A spectinomycin resistance cassette derived from pHP45Ω, flanked by short inverted repeats containing transcription and translation termination signals (37) on a SmaI fragment was subsequently inserted into the remaining unique HincII (pLH0679) or HpaI site (pLH0680) (Fig. 2), producing plasmids pLH0679Ω and pLH0680Ω, respectively. A gentamicin resistance cassette derived from pDAH346 (courtesy of D. Hodgson; see also reference 35) was inserted into pLH1247 at the unique SmaI site (Fig. 2), producing plasmid pLH1247lit38GN. Constructs were sequenced to confirm the integrity of the flanking DNA cloned and the orientation of the antibiotic cassette. Transformation of WT *Synechocystis* with these plasmid constructs was performed as described by Williams (53); see Table 2 for a full list of strains generated.

Whole-gene-cluster deletion mutants. The Δ*pst1* and Δ*pst2* in-frame, whole-gene-cluster deletion mutants were constructed using λ Red-mediated recombination (22). The *pst1* and *pst2* gene clusters were amplified by PCR using primers *pst1*exF (5′-GCGGGTCCAAACCGACTAAC-3′), *pst1*exR (5′-CGGCAATAG GGCGAGGATAC-3′), *pst2*exF (5′-TTTCCTCTTCGCCTTCTTGG-3′), and *pst2*exR (5′-CTTGCAGGGCAATAAACTCC-3′) and the following PCR conditions: an initial denaturation step at 95°C for 2 min, followed by 25 cycles of 98°C for 20 s, 45°C for 15 s, and 68°C for 4 min, followed by a final extension of 68°C for 5 min. Each 50-μl PCR mix contained 0.3 mM deoxynucleoside triphosphates (dNTPs), 0.3 μM primers, 100 ng *Synechocystis* genomic DNA, 1 U KAPAHiFi DNA polymerase, and 1× KAPAHiFi reaction buffer. PCR products were then ligated into the pGEM-T Easy vector (Promega, United States), producing constructs pITT*pst1* and pITT*pst2*. These plasmids were then electroporated into *E. coli* BW25113 containing the λ Red recombination plasmid pIJ790 (15). For each gene cluster disruption, PCR primers were then designed to specifically amplify the apramycin resistance cassette from plasmid pIJ773 (22). Each primer contains at the 5′ end 39 bp matching the *Synechocystis* chromosomal DNA sequence directly adjacent to the cluster to be inactivated. For the forward primer, the last 3 bp of the 39 bp corresponds to the start codon of the first gene of the cluster, and for the reverse primer, the stop codon for the last gene of the cluster. The remaining 19 bp of the primer corresponds

TABLE 1. Comparison of PstS and SphX P_i-binding protein properties in freshwater and marine cyanobacteria

Protein and gi no.	Organism[a]	Length[b]	SigP[c]	Mol wt[d]	pI[e]	Open reading frame
Freshwater and marine cyanobacterial PstS						
16331543	***Synechocystis* PCC 6803 (PstS1)**	**383**	**28 (1)**	**37,030**	**4.08**	***sll0680***
86604859	*Synechococcus* OS-A	349	23 (2)	35,095	4.28	
86610205	*Synechococcus* OS-B′	366	25 (3)	36,610	4.32	
86606387	*Synechococcus* OS-A	353	25 (3)	35,566	4.43	
86609371	*Synechococcus* OS-B′	353	25 (3)	35,767	4.61	
87123371	*Synechococcus* RS9917	337	28 (2)	32,142	4.88	RS9917_05910
33867037	*Synechococcus* WH8102	336	32 (2)	31,880	4.9	SYNW2507
17232067	*Anabaena* PCC 7120	392	30 (3)	38,083	5.02	*all4575*
37521603	*Gloeobacter* PCC 7421	349	33 (2)	33,594	6.06	*gll2034*
87124682	*Synechococcus* RS9917	340	24 (3)	33,327	6.79	RS9917_00632
26110901	*Escherichia coli*	346	25 (3)	34,408	7.46	
86608555	*Synechococcus* OS-B′	358	35 (2)	34,955	8.67	
86606216	*Synechococcus* OS-A	359	28 (2)	35,923	9.31	
37520014	*Gloeobacter* PCC 7421	347	31 (3)	33,983	9.44	*glr0445*
33866347	*Synechococcus* WH8102	325	25 (3)	31,479	9.65	SYNW1815
33241024	*Prochlorococcus* SS120	329	17 (1)	32,785	10.12	Pro1575
33240982	*Prochlorococcus* SS120	330	17 (2)	32,636	10.27	Pro1533
33861267	*Prochlorococcus* MED4	323	24 (3)	31,530	10.37	PMM0710
16330429	***Synechocystis* PCC 6803 (PstS2)**	**333**	**28 (3)**	**32,527**	**10.46**	***slr1247***
33865552	*Synechococcus* WH8102	324	24 (3)	31,475	10.54	SYNW1018
17228406	*Anabaena* PCC 7120	347	33 (3)	33,965	10.6	*all0911*
87124221	*Synechococcus* RS9917	326	24 (3)	31,278	10.72	RS9917_11445
Freshwater and marine cyanobacterial SphX						
16331544	***Synechocystis* PCC 6803 (SphX)**	**328**	**27 (1)**	**33,002**	**4.26**	***sll0679***
16331706	***Synechocystis* PCC 6803**	**307**	**22 (2)**	**30,385**	**4.54**	***sll0540***
87124691	*Synechococcus* RS9917	347	29 (2)	35,298	5.12	RS9917_00677
37519584	*Gloeobacter* PCC 7421	338	23 (2)	34,559	7.48	*glr0015*
37519581	*Gloeobacter* PCC 7421	337	22 (2)	34,576	7.6	*glr0012*
37519583	*Gloeobacter* PCC 7421	335	22 (1)	33,751	8.13	*glr0014*
37519577	*Gloeobacter* PCC 7421	340	32 (3)	33,563	8.84	*glr0008*
17228589	*Anabaena* PCC 7120	352	24 (1)	35,978	9.02	*alr1094*
17232077	*Anabaena* PCC 7120	309	None (3)	33,403	9.09	*alr4585*
86609984	*Synechococcus* OS-B′	335	27 (1)	32,849	9.51	
37519582	*Gloeobacter* PCC 7421	343	26 (3)	34,701	9.6	*glr0013*
86605896	*Synechococcus* OS-A	337	35 (1)	33,033	9.69	
33865820	*Synechococcus* WH8102	345	29 (2)	35,349	9.89	SYNW1286
37520552	*Gloeobacter* PCC 7421	384	79 (1)	32,273	10.09	*glr0983*
87124426	*Synechococcus* RS9917	355	32 (3)	36,068	10.38	RS9917_12470
37519585	*Gloeobacter* PCC 7421	387	84 (1)	32,686	10.55	*glr0016*

[a] *Synechocystis* data are in bold.
[b] Length of the native protein (number of amino acid residues).
[c] Signal peptide cleavage site as predicted *in silico*. The number in parentheses is the number of algorithms, out of three used, predicting this site.
[d] Molecular weight of the mature polypeptide.
[e] Isoelectric point of the mature polypeptide.

to the 5′ or 3′ end of the apramycin disruption cassette. The PCR primers used for amplification of the apramycin resistance cassette to be inserted into *pst1* were *pst1*redF (5′-AAAGCTACCGTCAACGGCTAATCACAATCGACCACCCTGGGGGCGGAGAAGTAAAA**ATG**ATTCCGGGGATCCGTCGACC-3′) and *pst1*redR (5′-RCTTTTGGATTTATTTAATTTCACCAACTTGATTTAATTAGTTAATTGACAGTTAA**TTA**TGTAGGCTGGAGCTGCTTC-3′). For amplification of the apramycin resistance cassette to be inserted into *pst2*, the primers were *pst2*redF (5′-TCAGCGAACAAGGGCTGACTGTTTCAACTGCACTACAATTTAGATTGCAAATTCCT**ATG**ATTCCGGGGATCCGTCGACC-3′) and *pst2*redR (5′-TAAGAGGTAATACAAGCAAACGTTATATGAAGGAGGGCACCATAAACAGGAGTAT**CTA**TGTAGGCTGGAGCTGCTTC-3′) (the start and stop codons are highlighted in bold, and the sequence corresponding to the antibiotic resistance cassette is underlined). Each 50-μl PCR mix contained 0.3 mM dNTPs, 0.5 μM primers, 100 ng pIJ773, 5% (vol/vol) dimethyl sulfoxide (DMSO), 2 U KAPAHiFi DNA polymerase, and 1× KAPAHiFi reaction buffer. PCR conditions were as follows: 94°C for 2 min, followed by 94°C for 45 s, 50°C for 45 s, and 72°C for 90 s repeated for 10 cycles, followed by 94°C for 45 s, 55°C for 45 s, and 72°C for 90 s repeated for 15 cycles, followed by a final extension of 72°C for 5 min. PCR products were transformed into *E. coli* BW25113 grown in LB containing 10 mM arabinose. Subsequent constructs were sequenced to confirm the correct in-frame insertion of the antibiotic resistance cassette before transformation into *Synechocystis*. *Synechocystis* transformants were selected in BG-11 solid medium supplemented with apramycin (50 μg ml^{-1}). Apramycin-resistant transformants were then grown in liquid BG-11 medium supplemented with 50 μg ml^{-1} apramycin.

Genomic DNA extraction. Extraction of *Synechocystis* genomic DNA from WT and mutant strains was carried out by using a method modified from Murray and Thompson (34) as described by Eguchi et al. (17) and by using 20 to 30 ml of early-logarithmic-phase culture.

Confirmation of mutant segregation. To test whether *Synechocystis* mutant strains were completely segregated, i.e., homogeneous for the mutant chromosomes, PCR amplification with genomic DNA from the mutants as templates and the corresponding primers was carried out. For the whole-gene-cluster deletion mutants, the following PCR primers were designed to amplify an internal region of *pst1* or *pst2* in order to confirm complete loss of the WT region: *pst1*inF (5′-GCCTGTACACCATCCCAGAC-3′), *pst1*inR (5′-TCCCGAGTCGATTCC

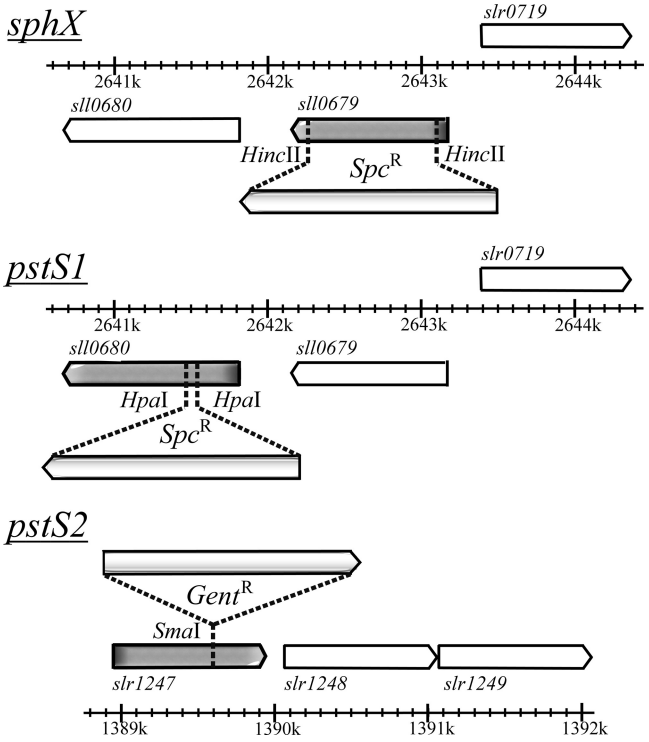

FIG. 2. Insertional mutagenesis of *Synechocystis sphX*, *pstS1*, and *pstS2*. Spc, spectinomycin; Gent, gentamicin.

TTGAG-3′), *pst2*inF (5′-CTCCGTAGTCAGCGTTATCG-3′), and *pst2*inR (5′-AACTGACCGATACGGCTTTC-3′).

Flow cytometry. Samples for flow cytometry were fixed in 0.2% (vol/vol) glutaraldehyde (grade II; Sigma) and stored at 4°C until analysis. *Synechocystis* cell abundance was determined in triplicate using a FACScan flow cytometer and CellQuest version 3.3 software (Becton Dickinson, San Jose, CA).

AP assay. Alkaline phosphatase (AP) activity was measured with the *para*-nitrophenyl phosphate (*p*NPP) assay (5), modified for use in a microplate reader (33).

Total RNA extraction and cDNA synthesis. RNA was extracted from *Synechocystis* by using a "hot-phenol" method (3) as modified by Scanlan et al. (39). Contaminating DNA was removed by treating samples with 8 U Turbo DNase (Ambion), and samples were further purified by passage through an RNeasy Mini column (Qiagen). mRNA quality was assessed by visual inspection using an Agilent 2100 Bioanalyzer (Agilent Technologies), and samples passed if they achieved an RNA integrity number (RIN) of >7.8. Quantification of mRNA used a NanoDrop ND-1000 UV-visible light spectrophotometer. cDNA synthesis was carried out using TaqMan reverse transcription reagents (ABI) following the manufacturer's guidelines. Each 100 μl of reaction mix contained 800 ng of total RNA, to which final concentrations of 2.5 μM random hexamers, 500 μM each dNTP, and 6.0 mM $MgCl_2$ were added. MultiScribe reverse transcriptase (3 U), RNase inhibitor (0.4 U), and 10 μl of 10× MultiScribe reverse transcriptase buffer were also added. Amplification of cDNA was carried out for 10 min at 25°C, 60 min at 42°C, and 5 min at 95°C in a Biometra T-gradient PCR thermal cycler.

Quantitative PCR using SYBR green. A single-well qPCR assay was used to quantify the expression of specific genes throughout each time course by using SYBR green as the reporting system. PCR primers were designed for cDNAs derived from transcripts of various putatively P_i-regulated genes as well as the housekeeping gene *rnpB* (Table 3). The qPCRs were performed using AmpliTaq Gold SYBR green universal PCR master mix (ABI) according to the manufacturer's guidelines. Each reaction was performed in a 25-μl volume in a MicroAmp Optical 96-well reaction plate with optical adhesive films for a cover. Each reaction volume contained 8 ng cDNA, 5 μM specific primer, and 1× AmpliTaq Gold SYBR green master mix. Reaction volumes were heated at 95°C for 10 min and then underwent 40 cycles of 95°C for 15 s and 62°C for 1 min, carried out on a model 7000 sequence detection system (Applied Biosystems). Each reaction was performed in triplicate for each gene at every time point sampled, allowing the mean threshold cycle (C_T) value to be calculated (11). C_T values were converted to gene copy number per ng of template cDNA in a 4-stage process, which involved the modification of the standard $2^{-\Delta\Delta CT}$ equation (4) as described by Clokie et al. (11). For the $2^{-\Delta\Delta CT}$ equation to be valid, the efficiency of amplification for each target gene and calibrator must be approximately equal to the efficiency of the reference amplification. To ensure that this was the case, the ΔC_T value was plotted for a range of cDNA template dilutions (from 10 to 0.3 ng) against log input cDNA concentration for each primer (data not shown). For each primer tested, the value of the regression (ΔC_T versus cDNA concentration) was less than 0.1, indicating approximately equal amplification efficiencies.

P_i radiotracer uptake. P_i uptake was initiated by the addition of 100 μl of a specific concentration of P_i containing tracer levels of $K_2H[^{32}P]O_4$ to 20 ml P_i-stressed culture (see above) containing approximately 7.5×10^7 cells ml^{-1}. Uptake was stopped by filtering 500 μl of cells through a 0.2-μm Minisart disposable filter (Sartorius). Samples were taken at 6 s, 12 s, 20 s, 30 s, 1 min, 5 min, and 10 min. Filtrate (200 μl) was then added to 4 ml of scintillant material (Ultima Gold; PerkinElmer) and mixed, and the outer surfaces of the vials were wiped with methanol impregnated tissue to remove any static charge prior to loading into the scintillation counter (Packard-Bell, United States). Total counts were recorded over 5 min (cpm) with a computerized correction factor applied. $^{32}P_i$ incorporation was calculated from the decrease in $^{32}P_i$ in the external medium at a range of P_i concentrations, 10 to 0.75 μM for the "high-range" uptake experiments and 250 to 15.6 nM for the "low-range" uptake experiments. To account for nonspecific adsorption, killed-cell controls (i.e., following the addition of 10 mM $HgCl_2$) were analyzed at each time point and P_i concentration, and any counts measured were subtracted from experimental samples. P_i uptake rates were normalized to cell abundance as determined by flow cytometry (see above). Kinetic parameters (V_{max} and K_s) were determined using the iterative rectangular hyperbolic curve-fitting procedure in Sigma Plot 8.0. The K_s and

TABLE 2. Strains used in this study

Strain	Description[a]	Reference or source
Synechocystis sp. PCC 6803	Wild-type strain	38
Synechocystis 0679mut	*Synechocystis* mutant containing a spectinomycin resistance cassette inserted into *sll0679* in the same orientation as the ORF	This work
Synechocystis 0680mut	*Synechocystis* mutant containing a spectinomycin resistance cassette inserted into *sll0680* in the same orientation as the ORF	This work
Synechocystis 1247mut	*Synechocystis* mutant containing a gentamicin resistance cassette inserted into *slr1247* in the same orientation as the ORF	This work
Synechocystis Δ*pst1*	*Synechocystis* mutant containing an apramycin resistance cassette replacing the *pst1* gene cluster (*sll0679*, *sll0680*, *sll0681*, *sll0682*, *sll0683*, and *sll0684*) in the same orientation as the ORF	This work
Synechocystis Δ*pst2*	*Synechocystis* mutant containing an apramycin resistance cassette replacing the *pst2* gene cluster (*slr1247*, *slr1248*, *slr1249*, and *slr1250*) in the same orientation as the ORF	This work

[a] ORF, open reading frame.

TABLE 3. Quantitative PCR oligonucleotide primers used in this study

Gene name (open reading frame)	Primer name	Sequence (5′–3′)	Amplicon length (bp)
sphX (*sll0679*)	0679F	TCGAAGAGCTAAAGCGCATTT	61
	0679R	TGGTTCCAGCGGGTCAAG	
pstS1 (*sll0680*)	0680F	GCCATGGACGACGAAGAGA	62
	0680R	GCGGTCATGGGAAGCATT	
pstC1 (*sll0681*)	0681F	CCGGTGGGAAACCATTTTTC	65
	0681R	ATAATCCCCCCGACAATGC	
pstS2 (*slr1247*)	1247F	AGCGGCAACGGTTAAGCA	67
	1247R	GTTACGGCGGGCAAAGGT	
pstC2 (*slr1248*)	1248F	CTGGTGGCGGGATTGGT	64
	1248R	ATGTCCCGGCTGATGGAA	
phoA (*sll0654*)	0654F	GAATTTGATGTCCGAATCCAAAA	65
	0654R	GGCCCAGTGGAATCAATAACA	
nucH (*sll0656*)	0656F	GCTACTTCAGAAGGGATTTTCATCTT	71
	0656R	ACCTTGTCGCCAACGTTAACA	
rnpB (*slr1469*)	1469F	GCGCACCAGCAGTATCGA	62
	1469R	CCTCCGACCTTGCTTCCAA	

V_{max} values presented in the text are the means of three independent experiments.

RESULTS

***Synechocystis* P_i-binding proteins.** The complete genome sequence of *Synechocystis* contains three potential PBP genes adjacent to associated ABC transporter components, namely, *sll0679* (encoding SphX), *sll0680* (encoding PstS1), and *slr1247* (encoding PstS2) (Fig. 1). In addition, *sll0540* encodes a fourth potential PBP that can also be identified by BLAST analysis, but it is flanked on the genome by genes encoding hypothetical proteins and is unlinked to an ATP transporter. Each putative PBP contains all/some of the key residues known to be critical for P_i binding in *E. coli* (30; data not shown). The PBPs have similar predicted molecular masses of 30 to 33 kDa, except PstS1, which is somewhat larger (37 kDa). In addition, three of the four PBPs have similar predicted isoelectric points (pIs) of 4 to 4.5, except PstS2, which has a predicted pI of 10.46. These ranges in predicted molecular masses and pIs essentially encompass the entire ranges in sizes and pIs of PBPs encoded in completed cyanobacterial genomes (Table 1). Phylogenetic analysis of PBPs demonstrated a clear separation of PBPs into either the archetypal PstS type or the SphX type (Fig. 3), the latter encompassing sll0679 and sll0540 proteins.

PBP gene expression during P_i stress. Expression levels of *sphX*, *pstS1*, *pstS2*, and *sll0540* as well as the proposed *pho* regulon genes *phoA* (*sll0654*; alkaline phosphatase gene) and *nucH* (*sll0656*; extracellular nuclease gene) were monitored over a 48-h time course during conditions of sufficient P_i and conditions of P_i stress. Under P_i-replete conditions, transcript levels of all genes were relatively stable and did not fluctuate more than 2-fold (Fig. 4). Transcript levels at 48 h were used as a reference, and all subsequent fold changes in gene expression were compared to the value at this time point. While gene expression levels did not change significantly under P_i-replete conditions, it is important to note that expression levels of *pstS1* (4.3×10^4 transcripts per ng of cDNA template) and *pstC1* (3.2×10^4 transcripts per ng of cDNA template) were an order of magnitude higher than those of all of the other genes. Eight hours after transfer into P_i stress conditions, the expression levels of virtually all the genes analyzed increased significantly (Fig. 4), peaking approximately 48 h after transfer. The exception was *sll0540*, which showed only a minor (3-fold) increase in gene expression 48 h after transfer. No temporal difference in the induction of *sphX*, *pstS1*, or *pstS2* gene expression was observed. However, strikingly, *pstS2* underwent a >300-fold increase in its expression, with transcript numbers reaching 1.1×10^6 transcripts per ng of cDNA template, similar to those of *pstS1*. While *phoA* and *nucH* gene expression levels were unchanged during P_i-replete growth, following transfer to P_i stress conditions, expression increased over 250-fold and 120-fold, respectively. Concomitant measurement of AP activity (see Fig. 7A) showed induction kinetics similar to those measured by the *phoA* gene expression data.

PBP gene expression during nitrogen and high-light stress. In order to assess whether the PBPs were differentially regulated by environmental factors other than P_i, we also followed gene expression following transfer to N stress conditions, or following a shift to high light intensity. While expression levels of *sphX*, *pstS1*, *pstS2*, *phoA* and *nucH* all increased following transfer to N stress conditions (Fig. 4), the maximum fold increases for nearly all genes analyzed were substantially lower (range, 5.6- to 25.8-fold lower). The exception was *sphX*, with transcript levels 1.7-fold greater than those observed during P_i stress conditions. Transfer to high-light conditions caused a rapid increase in expression of virtually all the *pho* regulon genes (Fig. 4), but this response was transient, with maximum transcript levels peaking at 6 h exposure and then generally returning to prestress levels by 24 h. The exceptions were *pstC2* and *pstC1*, whose expression levels slightly increased and decreased, respectively.

Construction and gene expression analysis of PBP interposon mutants. To determine the precise functional role of individual PBPs (except that encoded by *sll0540*, which showed no obvious induction of gene expression during P_i conditions and hence was not further analyzed), interposon mutants in each of the corresponding genes were constructed (Fig. 2). Confirmation of complete segregation of each mutant was verified by PCR (Fig. 5A). Both the *sphX* and *pstS2* mutants retained their ability to respond to change in external P_i. Thus,

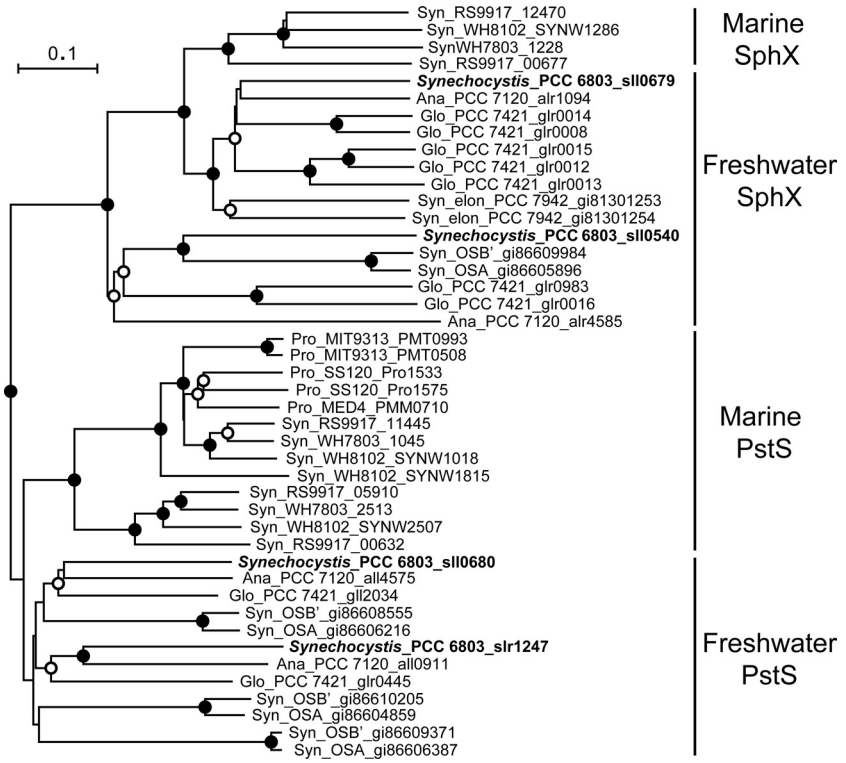

FIG. 3. Neighbor-joining tree based on the amino acid sequences of the mature PstS and SphX from marine and freshwater cyanobacteria. *Synechocystis* sequences are marked in bold. Syn, *Synechococcus*; elon, *elongatus*; Ana, *Anabaena*; *Gloeobacter*; Pro, *Prochlorococcus*. The tree was constructed from an alignment by using ClustalX v1.83. The bootstrap values were obtained through 1,000 repetitions, ● indicates a value of >95%, and ○ indicates a value of >50%. The tree is rooted on the PstS sequence of *Escherichia coli*. The scale bar represents 0.1 substitutions per amino acid.

transcript levels of *pho* regulon genes were similar to the WT levels under P_i-replete conditions (time point, −1 h; Fig. 6) but following transfer to P_i stress conditions increased as for the WT, though maximum fold increases were slightly lower. Exceptions to these trends were the elevated levels of *pstC2* in the *sphX* mutant, while in the *pstS2* mutant, levels of *pstC2* remained low and levels of *pstC1* increased to 4-fold higher than that in the WT (Fig. 6). However, in the *pstS1* mutant, high and constitutive levels of *sphX*, *pstS2*, *pstC2*, *phoA*, and *nucH* gene expression were observed irrespective of growth conditions (Fig. 6), suggesting an inability to regulate *pho* regulon gene expression in response to the external P_i concentration. Levels of *pstC1* transcript were also constitutively expressed in this mutant but at a considerably lower level than for the WT. AP activity measurements (Fig. 7B) mirrored *phoA* gene expression levels in each of the PBP mutants.

Transformation incompetence of the *pstS1* mutant. Attempts to complement the *pstS1* mutant by using a plasmid created for the insertion of WT *pstS1* into the *psbAII* gene or control transformations using a disruption construct for a non-*pho*-regulon-related gene were repeatedly unsuccessful, despite successful transformation of WT cells with an average efficiency of 1.8×10^3 transformants/μg DNA. This loss of natural transformation capacity was confirmed in five further independent *pstS1* disruption mutants, despite increasing the amount of plasmid from 1 to 10 μg in the transformation mix. Indeed, incubating *pstS1* cells with 2 μg of plasmid DNA showed no significant degradation of the added DNA even after 5 h of incubation (data not shown). Interestingly, this loss of transformation capacity correlates with the high, and constitutive, expressions of *phoA* and *nucH* potentially producing high-level phosphatase and nuclease activities in the periplasm of the *pstS1* mutant.

Construction of *pst1* and *pst2* gene cluster deletion mutants. Δ*pst1* and Δ*pst2* mutants were created using λ Red-mediated recombination to assess the kinetic properties of individual ABC transporters. During mutant construction, the apramycin resistance cassette was inserted in frame, from the start codon of the first gene to the stop codon of the last gene of each transporter (see Fig. 1 for gene order), to minimize any downstream effects. Complete segregation of each mutant was again ascertained by PCR (Fig. 5B).

$^{32}P_i$ radiotracer uptake kinetics in *pst1* and *pst2* deletion mutants. $^{32}P_i$ uptake kinetics performed on Δ*pst1* and Δ*pst2* mutants as well as WT cells showed dramatic differences in half-saturation constant (K_s) values and maximum uptake velocities (V_{max}s) (Table 4). The Δ*pst1* mutant had a >50-fold higher affinity for P_i than the Δ*pst2* mutant did, whereas the V_{max} for the Δ*pst2* mutant was 35-fold greater than that for the Δ*pst1* mutant. The *Synechocystis* WT strain demonstrated differential uptake kinetics dependent on the P_i concentration range used, but values were generally consistent with those obtained for "individual" transporters, as evidenced in the *pst1* and *pst2* mutants.

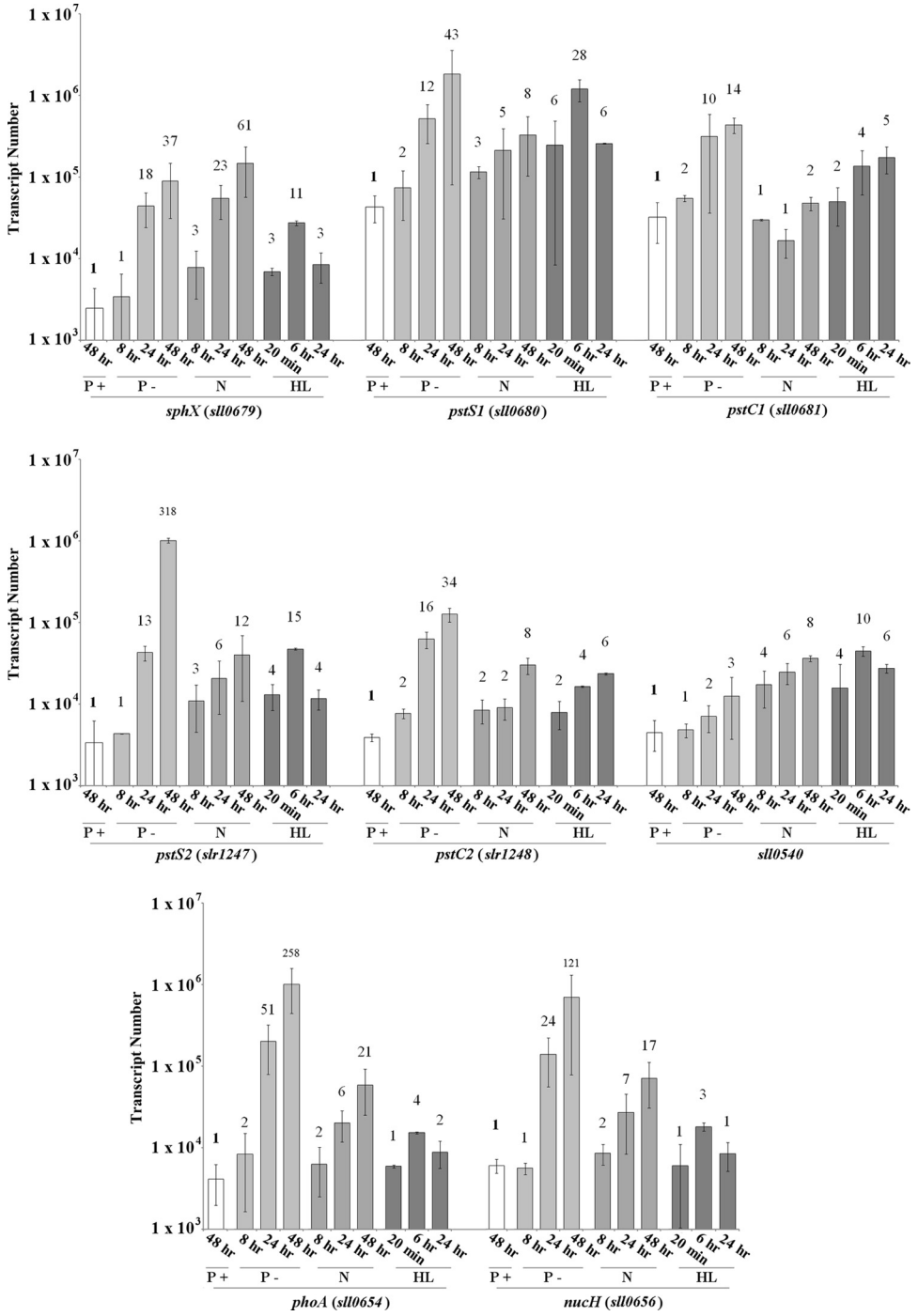

FIG. 4. Expression profiles of the *Synechocystis pho* regulon genes under P_i-replete (P+), P_i stress (P-), and N stress (N) conditions as well as following a shift to high light intensity (HL). Bar height indicates absolute transcript abundance per ng cDNA used in each qPCR. Numbers above each bar indicate fold change in gene expression compared to the gene transcript abundance at 48 h under P_i-replete conditions (indicated in bold).

AP activity in the *pstS1* interposon mutant and the *pst1* deletion mutant can be modulated. qPCR and AP activity data (Fig. 7B) showed that the *pstS1* mutant has high and constitutive AP levels. Such data were obtained following growth of the *Synechocystis* WT and the *pstS1* mutant in normal BG-11 medium, containing 420 μM P_i, for 48 h prior to washing and transfer to P_i stress conditions. To assess whether these alkaline phosphatase levels could be modulated, we exposed WT and mutant cells to 7.5 mM P_i (i.e., P_i excess) 12 h prior to transfer. Under such conditions, in the *pstS1* mutant, there was a >50% reduction in AP activity immediately following transfer compared to activity at 8 h (Fig. 8). Similarly, the *pst1* whole-gene-cluster deletion mutant showed a >35% reduction in activity at 0 h compared to that at 8 h. However, the extent

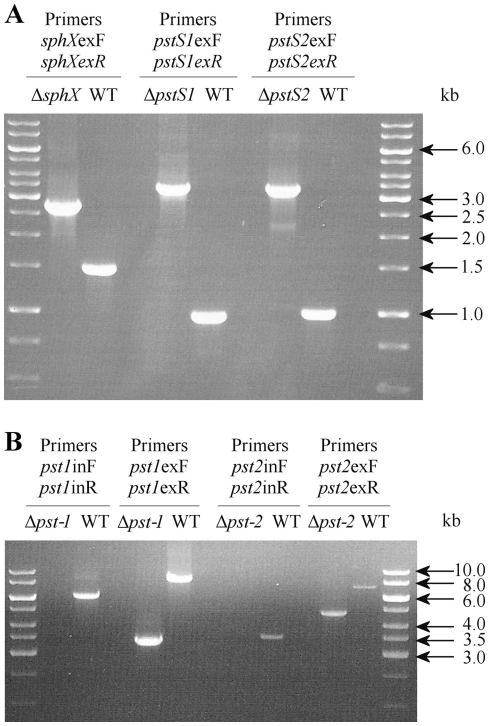

FIG. 5. PCR determination of the disruption of the targeted genes compared to *Synechocystis* WT. Data for *sphX*, *pstS1*, and *pstS2* (A) and *pst* (B) gene clusters are shown. This demonstrates that the disruption/deletion was obtained in all cases and that complete segregation occurred in each PBP and Δ*pst1* and Δ*pst2* mutants.

of this repression was still much lower than that for the WT, for which the activity was reduced >85%.

DISCUSSION

It is becoming increasingly apparent that cyanobacteria are not only able to thrive in environments with nanomolar concentrations of P_i but able to take advantage of periods of nutrient excess, forming extensive blooms in the ultimate stages of eutrophication (16). Such adaptability suggests that cyanobacteria possess a distinct competitive advantage when it comes to acquisition of P_i.

Genomic analyses demonstrate that a plethora of ABC transporters exists in cyanobacteria (40) and that, particularly in some freshwater strains, expansion and duplication of some of these systems have occurred (8). However, as yet, little work to elucidate the physiological role of such duplications or to identify any ecological advantages this may impart has been performed. P_i transport in *Synechocystis* is ideally placed as a model in this respect, since bioinformatic analyses have identified both duplicate ABC transporters and multiple associated binding proteins in this strain (43), while the organism is also readily genetically amenable (for an example, see reference 19), facilitating construction of specific transporter component mutants.

In this study, we attempted to answer two questions. First, is there a difference in function between the two putative P_i transporters, or is this simply functional "redundancy"? Second, within each P_i transporter, what is the role played by multiple and potentially redundant PBP components? In so doing, we also aimed to elucidate cellular control of specific P_i transporter components under a range of environmental variables.

To begin to address the first question, we compared gene expression profiles of P_i transporter components in WT cells grown under P_i-replete or P_i stress conditions. Strikingly, under growth with sufficient P_i, *pst1* transporter gene expression (represented by *pstC1* and *pstS1* transcript abundance) was on average 10-fold higher than that of *pst2*, i.e., as evidenced by *pstC2* and *pstS2* transcription (Fig. 4). However, shifting to P_i stress conditions caused dramatic (>300-fold) upregulations of *pstS2* gene expression and, to a lesser extent, *pstC2* (>40-fold), compared to the increases in *pstS1* (>50-fold) and *pstC1* (>20-fold), respectively. Thus, the individual P_i transporters appear to be differentially expressed as a function of the external P_i concentration. Subsequent construction of whole-gene-cluster deletion mutants and radiotracer uptake studies unequivocally demonstrated that each of the transporters has very different transport kinetic properties (Table 4), with a high-velocity, low-affinity Pst1 transporter contrasting with the low-velocity, high-affinity Pst2 transporter. Such biochemical information ties in nicely with the gene expression data, with high *pst1* expression under conditions of sufficient P_i facilitating a high rate of P_i uptake and allowing cells to take full advantage of an abundance of P_i (either by maintenance of a high growth rate or via luxury uptake and storage of P_i as polyphosphate; for an example, see reference 18). Under P_i stress conditions, *pstS2* and *phoA-nucH* gene expression levels increase substantially. Such induction of periplasmic or cell wall-associated enzymes capable of removing P_i groups from a wide variety of organic sources is typical for bacteria experiencing P_i stress (7, 27, 33, 48, 52) and is consistent with the elevated level of the PBP specific to this transporter facilitating maximal scavenging and delivery of P_i to *pst2* under stress conditions. Thus, possession of two P_i transporters gives *Synechocystis* the ability to extend the dynamic range over which P_i is acquired, potentially imparting a distinct ecological advantage over bacterial competitors.

The kinetic values reported here for the Pst1 and Pst2 transporters are within the range reported for other cyanobacteria (20, 21) and natural phytoplankton populations (12). However, much of the culture data relates to strains for which genome information is lacking, and hence, for which it is not known whether there is more than one P_i ABC transporter. Like that of *Synechocystis*, the genomes of hot spring *Synechococcus* sp. isolates OS-B′ and OS-A, *Anabaena variabilis*, *Anabaena* sp. strain PCC 7120, and *Gloeobacter violaceus* PCC 7421 also contain two potential P_i ABC transporters (43). Interestingly, phylogenetic analysis of the *Synechocystis*, *Anabaena*, and *Gloeobacter pstS* genes, which collectively describe a freshwater PstS clade (Fig. 3), contain two well-supported subclades, each containing a single PstS member from each strain. Hence, this might delineate biochemically divergent proteins with different binding affinities consistent with kinetic parameters for the whole transporter. In contrast, none of the genomes of any marine picocyanobacteria (40) or *Trichodesmium erythraeum* IMS101 (36, 43) contains two *pst* transporter gene clusters, although several contain multiple PBP gene homologs. This might indicate that in marine environments with persistently

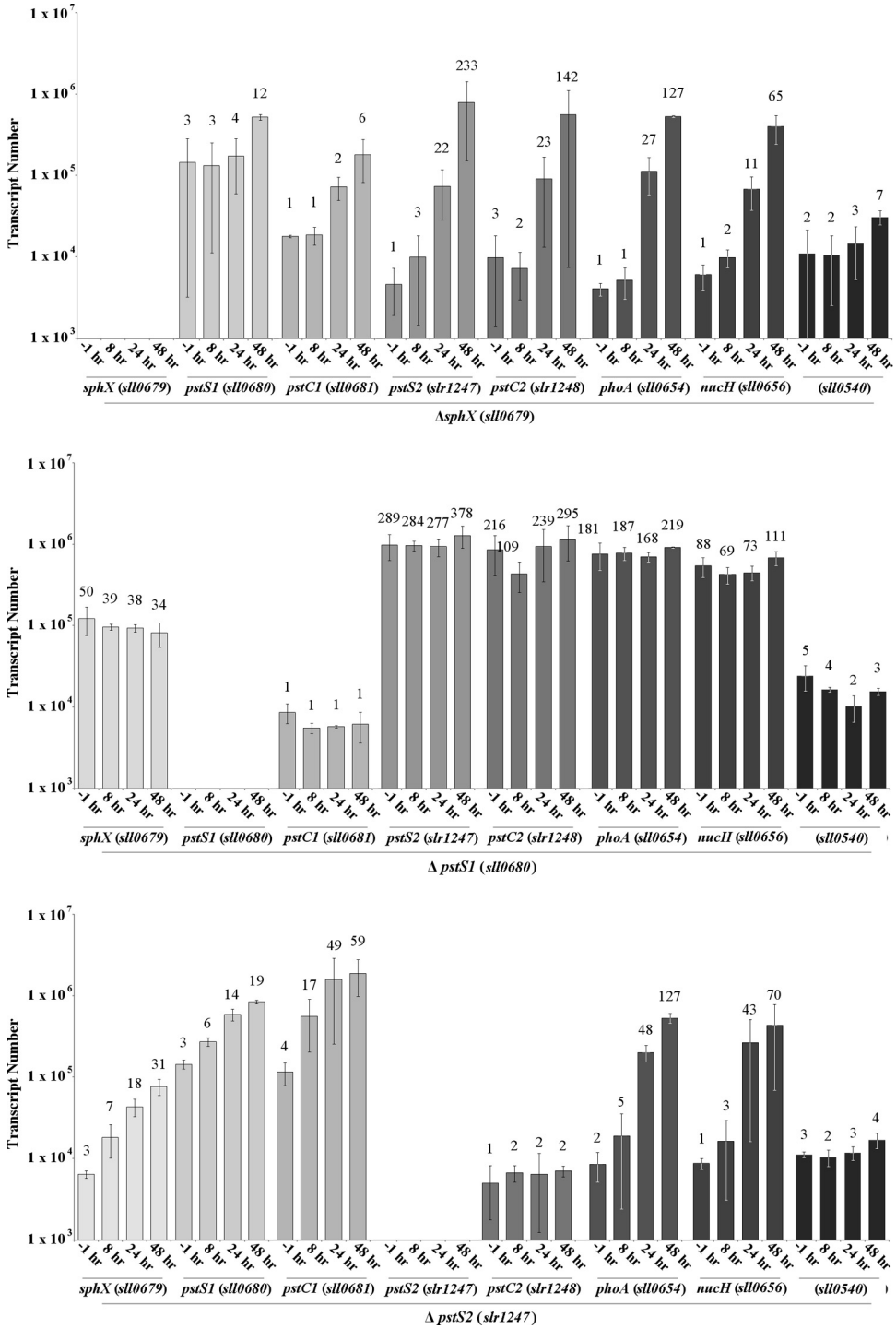

FIG. 6. Expression profiles of the *pho* regulon genes from *Synechocystis* PBP gene disruption mutants following transfer to P_i stress conditions. Bar height indicates absolute transcript abundance per ng cDNA used in each qPCR. Numbers above each bar indicate fold change in gene expression compared to the gene transcript abundance at 48 h under P_i-replete conditions (see Fig. 4).

low P_i concentrations, a single high-affinity Pst system has been selected for (see reference 1), in contrast to some freshwater environments where bioavailable P_i may fluctuate more frequently and over a greater concentration range, making it advantageous to have transporters with different kinetic and regulatory characteristics, as seen here with *Synechocystis*. However, it is also possible that the kinetic properties of even a single Pst system do differ subtly between strains, particularly if the multiple PBP components impart different P_i affinities. Indeed, in one freshwater *Synechococcus* organism, a single PBP possessed different P_i binding sites with dissociation constants in the micromolar and submicromolar ranges (50).

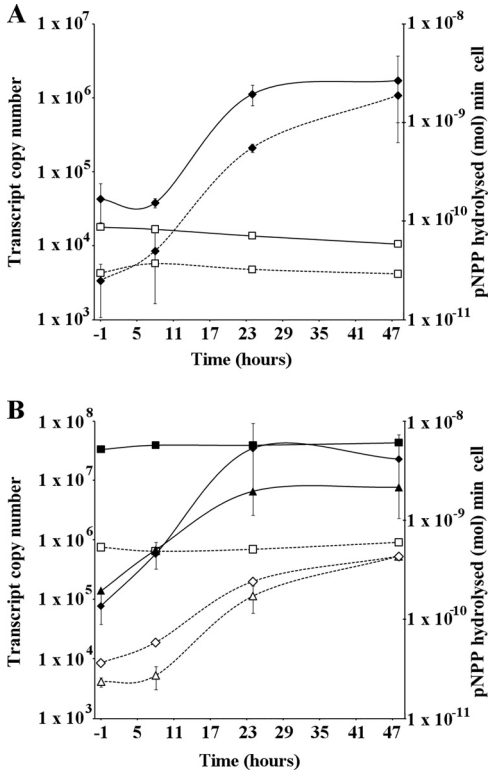

FIG. 7. AP activity (solid lines) and *sll0654* gene expression (dashed lines). (A) WT *Synechocystis* following transfer from P_i-replete to P_i stress conditions. □, P_i-replete conditions; ◆, P_i stress conditions. (B) *sphX*, *pstS1*, and *pstS2* disruption mutants following transfer from P_i-replete to P_i stress conditions. Squares, *pstS1* mutant; diamonds, *pstS2* mutant; triangles, *sphX* mutant. All AP assays were performed in triplicate. Error bars indicate maximum standard deviations observed.

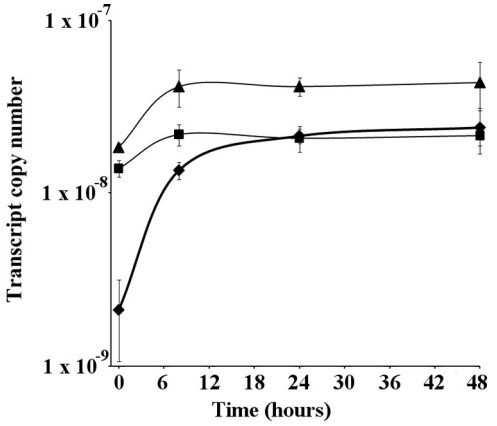

FIG. 8. AP activity in WT, *pstS1*, and *pst1* mutants following transfer from P_i-replete to P_i-stress conditions. ◆, WT; ▲, *pstS1* mutant; ■, *pst1* mutant. All AP assays were performed in triplicate. Error bars indicate the standard deviations of three replicates.

Extending comparison of the different kinetic properties of the *Synechocystis* Pst1 and Pst2 transporters more broadly, it is perhaps not surprising that most cyanobacterial genomes so far analyzed lack orthologs of the low-affinity Pit transporter found in *E. coli*, given that the half-saturation constant for the *E. coli* Pit transporter is 38 μM (55). Such a transporter would be ineffective in acquiring sufficient P_i to sustain cell growth at the levels generally found in freshwater systems.

After obtaining evidence for the differing kinetic properties of the two Pst transporters, we sought to examine the role of specific PBP components. qPCR data clearly demonstrated differential expressions of *sphX* and *pstS1* within *pst1*, with fold increases in *sphX* expression about 40% less than that of *pstS1*. Such differential regulation is consistent with computational prediction (43) of a *pho* box located between *sphX* and *pstS1* that corresponds to the experimentally determined PyTTAAP yPy(T/A) repeats found by Suzuki et al. (45) to bind the P_i response regulator SphR, which could explain the different expression patterns. Variation in the expression patterns of distinct PBP components was also observed following a shift to high light intensity or transfer of *Synechocystis* to N stress conditions. The high-light shift caused a transient increase in PBP gene expression peaking at 6 h and then declining to almost prestress levels by 24 h. However, while expression of *pstS1* increased >25-fold, fold increases of *sphX* and *pstS2* expression levels were much lower, well below the values observed during P_i stress. This upregulation of *pstS1* (*sll0680*) has been previously reported (6) and is consistent with the suggestion that under high-light conditions, P_i acquisition cannot keep pace with the growth potential of the cell, leading the cell to perceive P_i stress. Such an idea is consistent with the *pho* regulon sensor kinase SphS containing a PAS domain, since such modules are known to monitor changing light levels or redox potential (45, 46).

Further demonstration of differential expression of PBP components occurred following transfer of *Synechocystis* to N stress conditions. While this caused only a small increase in *pstS1* and *pstS2* gene expression levels, *sphX* levels were >60% higher than even those achieved under P_i stress. Potential control of *sphX* gene expression by the N-regulatory network warrants further investigation, especially if this might provide evidence for coregulation of N and P_i acquisition.

Additional evidence for a distinct role of SphX compared to PstS1 (or PstS2) was provided by qPCR data for the PBP

TABLE 4. Kinetic parameters of P_i uptake in WT *Synechocystis* and *pst1* and *pst2* whole-gene-cluster deletion mutants[a]

Strain	High range (10–0.75 μM)		Low range (250–15 nM)	
	K_s (μM)	V_{max} (fmol cell^{-1} min^{-1})	K_s (μM)	V_{max} (fmol cell^{-1} min^{-1})
Wild type	3.26 ± 0.5	34.15 ± 3.66	0.24 ± 0.05	3.8 ± 0.75
Δ*pst1* mutant	—	—	0.07 ± 0.01	0.88 ± 0.11
Δ*pst2* mutant	3.7 ± 0.7	31.18 ± 3.96	—	—

[a] Maximum uptake rates (V_{max}) and half-saturation constants (K_s) were obtained from five independent experiments, each performed in triplicate. The standard deviations are indicated. Dashes indicate that no measurable P_i uptake occurred during the time frame of the experiment.

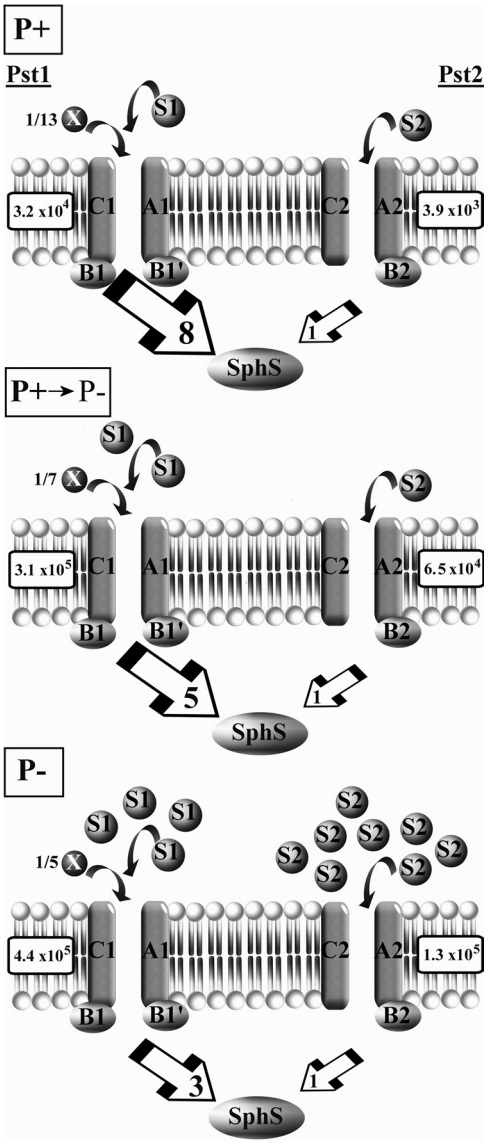

FIG. 9. Schematic model describing the abundance of each P_i transporter during a shift from P_i-replete (P+) to P_i stress (P-) conditions. The number of PBPs relative to each associated P_i transporter is calculated from the ratio of PBP to *pstC* transporter transcript abundance. Where this ratio is <1, a fraction adjacent to the PBP indicates its value. Large box arrows indicate the ratio of *pstC1* transcript abundance to *pstC2* transcript abundance. Transcript abundance values were taken at 48 h in P_i-replete conditions (P+) or 24 h (P+ → P-) or 48 h (P-) after transfer to P stress conditions (see Fig. 4). Boxed numbers adjacent to each P_i transporter represent actual *pstC1* or *pstC2* transcript abundance under each condition (see above).

disruption mutants upon transfer to P_i stress conditions. Thus, while the *sphX* and *pstS2* mutants showed upregulation of *pho* regulon genes similar to that of the WT, the *pstS1* mutant displayed high-level expression of *pho* regulon genes and high AP activity under both P_i-replete and P_i stress conditions, suggesting that the mutant had lost regulatory capacity and, hence, the ability to detect changes in external P_i. This suggests that *Synechocystis* primarily senses change in external [P_i] via the flow of P_i through PstS1 and interaction with its cognate Pst1 transporter to transmit a signal perceived by the sensor kinase SphS. However, providing P_i in excess prior to a shift to P_i stress conditions in either the *pstS1* mutant or the *pst1* whole-gene-cluster deletion mutant showed that AP activity could be modulated (Fig. 8), suggesting some regulatory capacity even in the absence of any *pst1* transporter component. Thus, it is possible that SphS is able to interact with both Pst1 and Pst2 to transmit a P_i stress signal but that this signal primarily derives from Pst1 and the level of P_i occupancy by PstS1 (Fig. 9). Such a model would be coherent with the observed expression levels of the Pst1 and Pst2 transporters during P_i-replete and P_i stress conditions. This model assumes that SphS interacts with a P_i ABC transporter component in a way similar to that of the *E. coli* P_i sensor PhoR, with PhoU acting as a negative regulator of the system (52). Indeed, recent evidence suggests that *Synechocystis sphU* (encoding a PhoU ortholog) plays a similar role (29) and that the extended N terminus of SphS is required for perception of P_i stress in *Synechocystis* (9).

ACKNOWLEDGMENTS

F.D.P. was the recipient of a NERC-funded Ph.D. studentship.

We thank M. Clokie for helpful discussions and analysis of the real-time PCR experiments, S. Bryan for providing assistance during the construction of the *Synechocystis* disruption mutants, and M. Ostrowski for critical reading of the manuscript.

REFERENCES

1. **Adams, M. M., M. R. Gomez-Garcia, A. R. Grossman, and D. Bhaya.** 2008. Phosphorus deprivation responses and phosphonate utilization in a thermophilic *Synechococcus* sp. from microbial mats. J. Bacteriol. **190:**8171–8184.
2. **Aiba, H., and T. Mizuno.** 1994. A novel gene whose expression is regulated by the response-regulator, SphR, in response to phosphate limitation in *Synechococcus* species PCC7942. Mol. Microbiol. **13:**25–34.
3. **Alley, M. R. K.** 1987. Molecular biological aspects of nitrogen starvation in cyanobacteria. Ph.D. thesis. Department of Biological Sciences, University of Warwick, Coventry, United Kingdom.
4. **Applied Biosystems.** 2001. User bulletin #2, ABI Prism 7700 sequence detection system. Applied Biosystems, Foster City, CA.
5. **Bessey, O. A., O. H. Lowry, and M. J. Brock.** 1946. A method for the rapid determination of alkaline phosphatase with five cubic millimeters of serum. J. Biol. Chem. **164:**321–329.
6. **Bhaya, D., D. Vaulot, P. Amin, A. W. Takahashi, and A. R. Grossman.** 2000. Isolation of regulated genes of the cyanobacterium *Synechocystis* sp. strain PCC 6803 by differential display. J. Bacteriol. **182:**5692–5699.
7. **Block, M. A., and A. R. Grossman.** 1988. Identification and purification of a derepressible alkaline-phosphatase from *Anacystis nidulans* R2. Plant Physiol. **86:**1179–1184.
8. **Bu, L., J. Xiao, L. Lu, G. Xu, J. Li, F. Zhao, X. Li, and J. Wu.** 2009. The repertoire and evolution of ATP-binding cassette systems in *Synechococcus* and *Prochlorococcus*. J. Mol. Evol. **69:**300–310.
9. **Burut-Archanai, S., A. Incharoensakdi, and J. J. Eaton-Rye.** 2009. The extended N-terminal region of SphS is required for detection of external phosphate levels in *Synechocystis* sp. PCC 6803. Biochem. Biophys. Res. Commun. **378:**383–388.
10. **Chan, F. Y., and A. Torriani.** 1996. PstB protein of the phosphate-specific transport system of *Escherichia coli* is an ATPase. J. Bacteriol. **178:**3974–3977.
11. **Clokie, M. R. J., J. Y. Shan, S. Bailey, Y. Jia, H. M. Krisch, S. West, and N. H. Mann.** 2006. Transcription of a 'photosynthetic' T4-type phage during infection of a marine cyanobacterium. Environ. Microbiol. **8:**827–835.
12. **Cotner, J. B., and R. G. Wetzel.** 1992. Uptake of dissolved inorganic and organic phosphorus compounds by phytoplankton and bacterioplankton. Limnol. Oceanogr. **37:**232–243.
13. **Currie, D. J.** 1990. Large-scale variability and interactions among phytoplankton, bacterioplankton, and phosphorus. Limnol. Oceanogr. **35:**1437–1455.
14. **Currie, D. J., and J. Kalff.** 1984. A comparison of the abilities of freshwater algae and bacteria to acquire and retain phosphorus. Limnol. Oceanogr. **29:**298–310.
15. **Datsenko, K. A., and B. L. Wanner.** 2000. One-step inactivation of chromosomal genes in *Escherichia coli* K-12 using PCR products. Proc. Natl. Acad. Sci. U. S. A. **97:**6640–6645.

16. **Dokulil, M. T., and K. Teubner.** 2000. Cyanobacterial dominance in lakes. Hydrobiologia **438:**1–12.
17. **Eguchi, M., M. Ostrowski, F. Fegatella, J. Bowman, D. Nichols, T. Nishino, and R. Cavicchioli.** 2001. *Sphingomonas alaskensis* strain AFO1, an abundant oligotrophic ultramicrobacterium from the North Pacific. Appl. Environ. Microbiol. **67:**4945–4954.
18. **Falkner, R., and G. Falkner.** 1989. Phosphate uptake by eukaryotic algae in cultures and by a mixed phytoplankton population in a lake—analysis by a force flow relationship. Bot. Acta **102:**283–286.
19. **Flores, E., A. M. Muro-Pastor, and J. C. Meeks.** 2008. Gene transfer to cyanobacteria in the laboratory and in nature, p. 45–57. *In* A. Herrero and E. Flores (ed.), The cyanobacteria: molecular biology, genomics and evolution. Caister Academic Press, Norfolk, United Kingdom.
20. **Fu, F. X., Y. H. Zhang, Y. Y. Feng, and D. A. Hutchins.** 2006. Phosphate and ATP uptake and growth kinetics in axenic cultures of the cyanobacterium *Synechococcus* sp. CCMP 1334. Eur. J. Phycol. **41:**15–28.
21. **Grillo, J. F., and J. Gibson.** 1979. Regulation of phosphate accumulation in the unicellular cyanobacterium *Synechococcus*. J. Bacteriol. **140:**508–517.
22. **Gust, B., G. Chandra, D. Jakimowicz, Y. Q. Tian, C. J. Bruton, and K. F. Chater.** 2004. λ Red-mediated genetic manipulation of antibiotic-producing *Streptomyces*. Adv. Appl. Microbiol. **54:**107–128.
23. **Hecky, R. E., and P. Kilham.** 1988. Nutrient limitation of phytoplankton in freshwater and marine environments—a review of recent evidence on the effects of enrichment. Limnol. Oceanogr. **33:**796–822.
24. **Hoffer, S. M., and J. Tommassen.** 2001. The phosphate-binding protein of *Escherichia coli* is not essential for P_i-regulated expression of the *pho* regulon. J. Bacteriol. **183:**5768–5771.
25. **Hudson, J. J., and W. D. Taylor.** 2005. Rapid estimation of phosphate at picomolar concentrations in freshwater lakes with potential application to P-limited marine systems. Aquat. Sci. **67:**316–325.
26. **Hulett, F. M.** 2002. *Bacillus subtilis* and its closest relatives: from genes to cells, p. 193–201. ASM Press, Washington, DC.
27. **Hulett, F. M., C. Bookstein, and K. Jensen.** 1990. Evidence for two structural genes for alkaline phosphatase in *Bacillus subtilis*. J. Bacteriol. **172:**735–740.
28. **Jackson, R. J., M. R. B. Binet, L. J. Lee, R. Ma, A. I. Graham, C. W. McLeod, and R. K. Poole.** 2008. Expression of the PitA phosphate/metal transporter of *Escherichia coli* is responsive to zinc and inorganic phosphate levels. FEMS Microbiol. Lett. **289:**219–224.
29. **Juntarajumnong, W., T. A. Hirani, J. M. Simpson, A. Incharoensakdi, and J. J. Eaton-Rye.** 2007. Phosphate sensing in *Synechocystis* sp. PCC 6803: SphU and the SphS-SphR two-component regulatory system. Arch. Microbiol. **188:**389–402.
30. **Luecke, H., and F. A. Quiocho.** 1990. High specificity of a phosphate-transport protein determined by hydrogen-bonds. Nature **347:**402–406.
31. **Makino, K., M. Amemura, S.-K. Kim, A. Nakata, and H. Shinagawa.** 1994. Mechanism of transcriptional activation of the phosphate regulon in *Escherichia coli*, p. 5–12. *In* A. Torriani-Gorini, E. Yagil, and S. Silver (ed.), Phosphate in microorganisms. ASM, Washington, DC.
32. **Mann, N. H., and D. J. Scanlan.** 1994. The SphX protein of *Synechococcus* sp. PCC7942 belongs to a family of phosphate-binding proteins. Mol. Microbiol. **14:**595–596.
33. **Moore, L. R., M. Ostrowski, D. J. Scanlan, K. Feren, and T. Sweetsir.** 2005. Ecotypic variation in phosphorus acquisition mechanisms within marine picocyanobacteria. Aquat. Microb. Ecol. **39:**257–269.
34. **Murray, M. G., and W. F. Thompson.** 1980. Rapid isolation of high molecular-weight plant DNA. Nucleic Acids Res. **8:**4321–4325.
35. **Nair, U., C. Thomas, and S. S. Golden.** 2001. Functional elements of the strong *psbAI* promoter of *Synechococcus elongatus* sp. PCC 7942. J. Bacteriol. **183:**1740–1747.
36. **Orchard, E. D., E. A. Webb, and S. T. Dyhrman.** 2009. Molecular analysis of the phosphorus starvation response in *Trichodesmium* spp. Environ. Microbiol. **11:**2400–2411.
37. **Prentki, P., and H. M. Krisch.** 1984. *In vitro* insertional mutagenesis with a selectable DNA fragment. Gene **29:**303–313.
38. **Rippka, R., J. Deruelles, J. B. Waterbury, M. Herdman, and R. Y. Stanier.** 1979. Generic assignments, strain histories and properties of pure cultures of cyanobacteria. J. Gen. Microbiol. **111:**1–61.
39. **Scanlan, D. J., N. H. Mann, and N. G. Carr.** 1993. The response of the picoplanktonic marine cyanobacterium *Synechococcus* sp. WH7803 to phosphate starvation involves a protein homologous to the periplasmic phosphate-binding protein of *Escherichia coli*. Mol. Microbiol. **10:**181–191.
40. **Scanlan, D. J., M. Ostrowski, S. Mazard, A. Dufresne, L. Garczarek, W. R. Hess, A. F. Post, M. Hagemann, I. Paulsen, and F. Partensky.** 2009. Ecological genomics of marine picocyanobacteria. Microbiol. Mol. Biol. Rev. **73:**249–299.
41. **Schindler, D. W.** 1977. Evolution of phosphorus limitation in lakes. Science **195:**260–262.
42. **Stanier, R. Y., and G. Cohen-Bazire.** 1977. Phototropic prokaryotes: the cyanobacteria. Annu. Rev. Microbiol. **31:**225–274.
43. **Su, Z. C., V. Olman, and Y. Xu.** 2007. Computational prediction of Pho regulons in cyanobacteria. BMC Genomics **8:**156.
44. **Surin, B. P., H. Rosenberg, and G. B. Cox.** 1985. Phosphate-specific transport system of *Escherichia coli*—nucleotide sequence and gene polypeptide relationships. J. Bacteriol. **161:**189–198.
45. **Suzuki, S., A. Ferjani, I. Suzuki, and N. Murata.** 2004. The SphS-SphR two component system is the exclusive sensor for the induction of gene expression in response to phosphate limitation in *Synechocystis*. J. Biol. Chem. **279:**13234–13240.
46. **Taylor, B. L., and I. B. Zhulin.** 1999. PAS domains: internal sensors of oxygen, redox potential, and light. Microbiol. Mol. Biol. Rev. **63:**479–506.
47. **Thompson, J. D., T. J. Gibson, F. Plewniak, F. Jeanmougin, and D. G. Higgins.** 1997. The ClustalX windows interface: flexible strategies for multiple sequence alignment aided by quality analysis tools. Nucleic Acids Res. **25:**4876–4882.
48. **Torriani-Gorini, A.** 1994. The pho regulon of *Escherichia coli*—introduction, p. 1–4. *In* A. Torriani-Gorini, E. Yagil, and S. Silver (ed.), Phosphate in microorganisms: cellular and molecular biology. ASM, Washington, DC.
49. **van Veen, H. W., T. Abee, G. J. J. Kortstee, W. N. Konings, and A. J. B. Zehnder.** 1994. Translocation of metal phosphate via the phosphate inorganic transport-system of *Escherichia coli*. Biochemistry **33:**1766–1770.
50. **Wagner, F., M. Gimona, H. Ahorn, G. A. Peschek, and G. Falkner.** 1994. Isolation and functional reconstitution of a phosphate-binding protein of the cyanobacterium *Anacystis nidulans* induced during phosphate-limited growth. J. Biol. Chem. **269:**5509–5511.
51. **Wanner, B. L.** 1993. Gene regulation by phosphate in enteric bacteria. J. Cell. Biochem. **51:**47–54.
52. **Wanner, B. L.** 1996. Phosphorus assimilation and control of the phosphate regulon, p. 1357–1377. *In* F. C. Neidhardt, R. Curtiss III, J. L. Ingraham, E. C. C. Lin, K. B. Low, B. Magasanik, W. S. Reznikoff, M. Riley, M. Schaechter, and H. E. Umbarger (ed.), *Escherichia coli* and *Salmonella*: cellular and molecular biology, 2nd ed. ASM Press, Washington, DC.
53. **Williams, J. G. K.** 1988. Construction of specific mutations in photosystem II photosynthetic reaction center by genetic engineering methods in *Synechocystis* sp. PCC6803. Methods Enzymol. **167:**766–778.
54. **Willsky, G. R., R. L. Bennett, and M. H. Malamy.** 1973. Inorganic phosphate transport in *Escherichia coli*: involvement of two genes which play a role in alkaline phosphatase regulation. J. Bacteriol. **113:**529–539.
55. **Willsky, G. R., and M. H. Malamy.** 1980. Characterization of two genetically separable inorganic phosphate transport systems in *Escherichia coli*. J. Bacteriol. **144:**356–365.